Design and performances of a turbo-electric and Distributed Propulsion aircraft in the Small and Medium Range segment: intermediate results from the European project IMOTHEP

Eric Nguyen Van* and Sebastien Defoort†
ONERA, Toulouse, France

Christophe Viguier‡
SAFRAN TECH, Blagnac, France

Smail Mezani§ and Noureddine Takorabet¶
GREEN, Université de Lorraine, F-54000, Nancy, France

Jesúz Sainz‖
ITP Aero, Alcobendas, Spain

This paper presents the intermediate results of the European project IMOTHEP: "Investigation and Maturation of Technologies for Hybrid Electric Propulsion". The IMOTHEP project aims at improving the evaluation of the potential of hybrid electric propulsion to reduce fuel consumption for both regional aircraft and Small and Medium Range (SMR) aircraft. This publication introduces the work performed on the SMR conservative (or SMR-CON) aircraft during the intermediate design loop. The SMR-CON is a tube and wing aircraft equipped with a turbo-electric architecture and Distributed Electric Propulsion. The intermediate design loop consisted in designing propulsive components based on the requirement derived from the initial design loop and integrating them in the overall aircraft design tool for the evaluation of performance and design sensitivities. Compared to the initial design loop, it was found that the first component designs reached a level of performance insufficient to show a benefit of a turbo-electric aircraft over a traditional UHBR turbofan aircraft in the SMR segment. Sensitivity analysis and decomposition of efficiency of the turbo-electric chain identifies possible ways of improvements among which the efficiency of the turbomachine is a key parameter.

I. Introduction

The IMOTHEP project « Investigation and Maturation of Technologies for Hybrid Electric Propulsion », gather more than twenty partners, studies four concept spanning two segments of transportation aircraft. In this first section, an introduction to the project and its goals is made, followed by a description of the aircraft concept studied in this paper.

A. The IMOTHEP project and the current design iteration

The main objective of the IMOTHEP project is to significantly improve the estimation of the potential offered by hybrid electric propulsion in order to reduce the fuel consumption and CO2 emissions of civilian transport aircraft [1]. Four hybrid aircraft configurations are studied and compared to a reference turbofan aircraft representative of actual technology levels and a baseline aircraft representative of technology levels for Entry Into Service (EIS) 2035.

The four configurations are split into two segments: (i) regional transport aviation (REG) and (ii) Small to Medium Range (SMR) transport aircraft. Within each segment, a conservative and a radical aircraft configurations are studied. The conservative configuration is named after its proximity with conventional "Tube and wing" aircraft while the radical

---

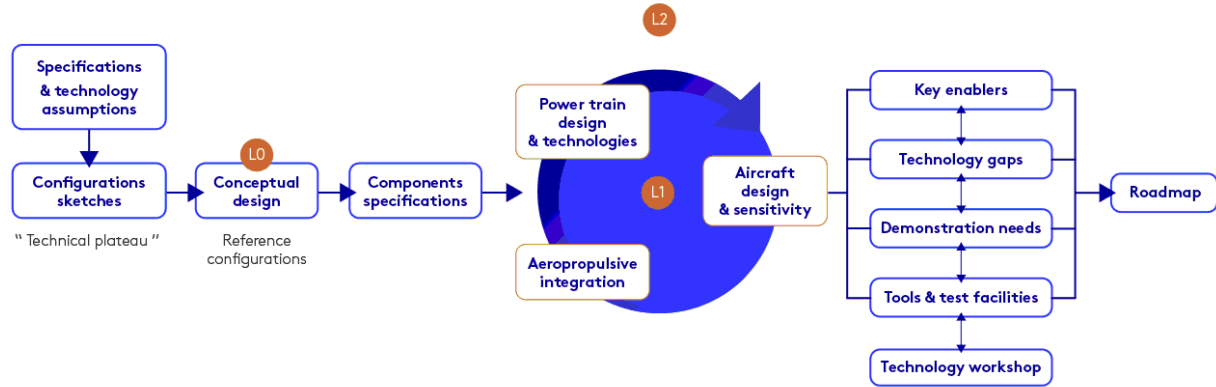*Research Engineer, DTIS, eric.nguyen_van@onera.fr
†Research Engineer, DTIS, sebastien.defoort@onera.fr.
‡Deputy of E&E Director, Senior Expert - Electrical Machines, E&E Departement
§Senior lecturer, Laboratory GREEN
¶Professor, Laboratory GREEN
‖Engine Performance Aerothermal and Systems.

Fig. 1   IMOTHEP's project approach

configuration explores more disruptive propulsion integration and aircraft layout (see [2] and [3] for more details on the radical aircraft).

This project gathers 27 European as well as Canadian partners and research institutes. Each partner brings an expertise in some of the many disciplines, from components modelling to overall aircraft evaluation, which are needed to model and analyse a hybrid electric propulsion aircraft. The work is organised in three design loops:

- L0 : first conceptual design loop, independent or loosely coupled multi-disciplinary evaluation from Top Level Requirements. For a presentation of the work accomplished during the L0 loop see [4].
- L1 : first multi-disciplinary design loop integrating models provided by different work-packages, especially models of hybrid electric components (electric motor, cables, converters, turboshaft, generator,. . .).
- L2 : second multi-disciplinary design loop integrating refined and higher fidelity models, and addressing transient effects.

The work presented in this paper is the outcome of the L1 design iteration that ended in January 2023. The results of this study are used to issue recommendations for the work that should be completed in Design Loop 2 (L2) where higher fidelity disciplinary analysis should be conducted on the most promising concept.

B. Introduction of the SMR-CON concept

Ultra High By Pass Ratio (UHBR) turbofan or Unducted Single Fan engines (USF) are viewed as the next major propulsive evolution to increase the fuel efficiency of civil transport aircraft [5]. However, the integration of new, larger and heavier engines on traditional aircraft is increasingly complicated as geometrical, structural or handling quality constraints are hit [6]. In IMOTHEP, the SMR-CON aircraft relies on the DRAGON concept which idea is to substitute a large diameter turbofan by many small and distributed electric fans powered by a turbomachine. The flexibility of electric motors in size and shape, while retaining an excellent efficiency, allows the distribution and better integration of the propulsion to the air-frame as well as providing an exceptionally large by-pass ratio.

The SMR-CON is based on a traditional tube&wing layout with the gaz turbine generators located at the rear. The electric fans are located at the trailing edge in the pressure side of the wing (see Fig 2). Such implementation was guided by the willingness to maintain a clean suction side so as to better manage the shock at transonic speeds. Boundary Layer Ingestion (BLI) was expected to bring little to no benefit at all and was not regarded as an objective for this concept.

The large surface area of the fans increases the by-pass ratio up to values of 40, well beyond what would be achievable with an UHBR engine. The propulsive efficiency is considerably increased, however it comes at the cost of additional losses in the electrical power transmission, added weight and additional challenges such as designing a safe power architecture and a heavy thermal management system. The integration of the electric fans under the wing, while still targeting a transonic cruise speed of Mach 0.78, also comes at a price in integration drag and added wetted surface area.

The concept was evaluated with an Overall Aircraft Design (OAD) tool in previous studies in [6], [7], [8] and [9] and despite the cost of installation of a hybrid electric propulsion chain, a better fuel efficiency was achieved with

**Fig. 2   The SMR-CON concept based on the DRAGON [6] aircraft**

reasonable projections on the performances of available technology for EIS2035. These assumptions are the weak point of these previous works: it requires the gathering and work of disciplinary specialists together with overall aircraft designers to estimate the performances of aircraft components with projected improvement up to 2035. Re-enforcing this aspect was identified as a future work, and this was the context in which the IMOTHEP project started.

To improve the estimation of the potential of hybrid electric propulsion to increase fuel efficiency, the large consortium gathers disciplinary specialists tasked with improving the expected technology projection in their respective field. The preliminary work realised for the Dragon concept furnishes a baseline design for all partners to quick start the work and an OAD environment readily available to evaluate the disciplinary solutions at the aircraft level. Compared to the Dragon concept, the SMR-CON benefits from inputs of disciplinary specialists taking care of electric power unit (electric motor and associated power electronic), turbomachine and thermal management system design.

II. Description of the design tool and sizing process

A. Multidisciplinary Design tool: FAST-OAD

The OAD tool used to analyse the SMR-CON aircraft is the software FAST-OAD [10]. FAST-OAD is an open source preliminary design tool created and maintained by both ONERA and ISAE-SUPAERO that comes with a set of semi-empirical models allowing to reproduce aircraft of the A320 family. The plugin architecture of FAST-OAD allows to construct any particular design process by adding or removing specific modules or submodules. Hence, the SMR-CON aircraft is modeled in FAST-OAD by adding a propulsion module to size the hybrid-electric architecture. Specific sub-models were then modified to account for the changes in geometry, aerodynamics (essentially additional wetted surface area) and most importantly weight and weight distribution. These additional modules were developed specifically for hybrid-electric propulsion and are not part of the open-source release of the software.
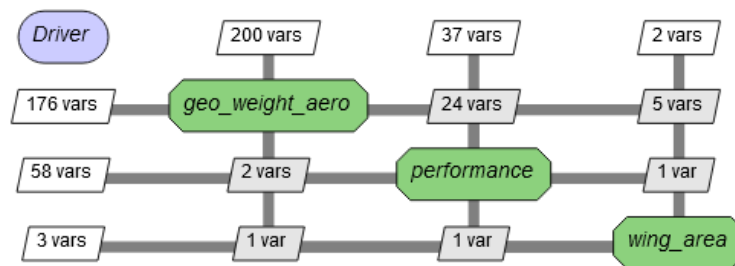
Fig. 3   Main XDSM scheme of the design process

Figure 3 shows the main design loop in three blocs where the aircraft is sized in the module "geo_weight_aero", evaluated in the module "performance" and the wing area is updated in the last bloc. Figure 4 shows the details of

sub-analysis "geo_weight_aero". The number of variables exchanged in between the blocs identifies couplings between the different disciplines.
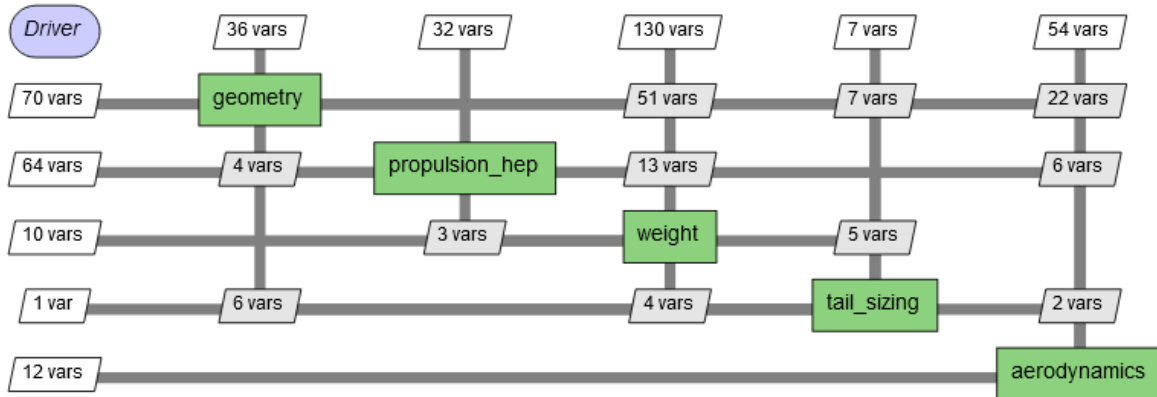

Fig. 4   Details of the bloc "geo_weight_aero".

FAST-OAD is built on the OpenMDAO [11] framework and takes advantage of the variable promotion and when available, the use of partial derivatives to speed up the resolution of multidisciplinary analysis and optimization.

B. Propulsive architecture

Previous work at ONERA initiated a reflection to provide high levels of safety with distributed propulsion [12]. The Hybrid Distributed Electric Propulsion (HDEP) architecture of the SMR-CON, illustrated in Fig5, was built on the outcome of this previous exercise. Although the number of components is subject to change, the interconnection methodology and the distribution of the components answer the same goals:
- To provide a cross-redundant electrical power distribution,
- To be robust to single component failure,
- To limit the oversizing of components.

The architecture features two turboshafts each mechanically coupled to two generators (GL and GR in Fig 5). Each generator is feeding two cores (Propulsion Bus DC + Fault Current Limiter + Breakers) in a cross-redundant DC connection. As such, if one generator or one turboshaft fails, all cores can be powered by the remaining turbomachine/generators. Finally, each core distributes power to a cluster of electric fans symmetrically arranged on the wings so that the loss of one core, translating in a loss of thrust, does not produce parasitic yawing moment.

This architecture being fully turbo-electric, it features no battery as source of energy. A small quantity of battery may still be used as buffer for handling transient dynamics and in this case, they are included in the cores.

The propulsion chain is sized starting from the efans which dimensions are fixed by the thrust requirement at Top Of Climb (TOC) conditions. The power of each components are then deduced from the propulsive efficiency of the efans and a set of thrust requirement taking into account the design mission requirements (see Table 17) and emergency situation such as One Turboshaft Inoperative, One Generator Inoperative and One Core Inoperative. Thanks to the redundancy of the turbo-electric architecture, none of these emergency situations are constraining. The components are generally sized by the Take-Off Field Length or the time to climb requirement. The reader is referred to [4] for details about the sizing flight conditions.

III. Description of the components designed during loop L1

A. Power units: turboshaft and generator

The workpackage dedicated to power generation delivered two components:
- a turbomachine for which a consumption map as a function of flight conditions and power level was provided as well as weight and size estimations.
- an electric generator for which efficiency, weight and size estimations where provided.
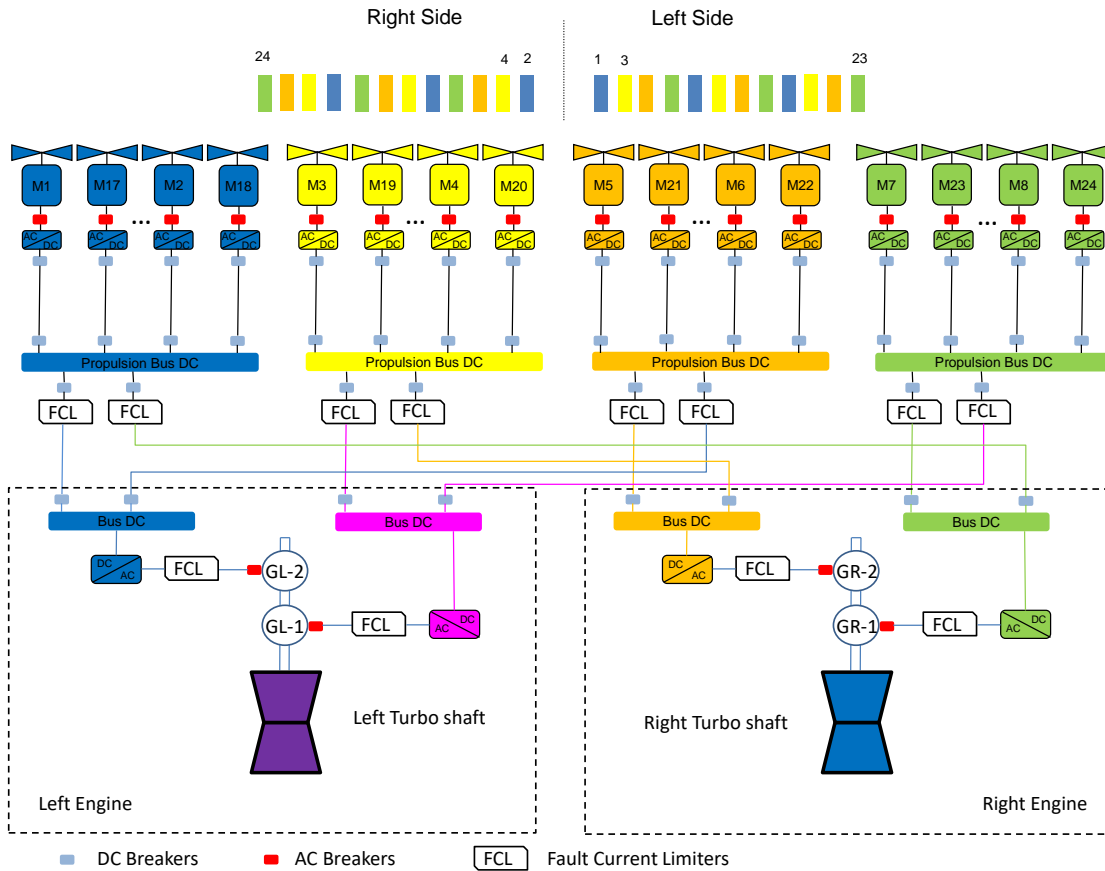
Fig. 5 turbo-electric propulsive architecture.

Both components have been designed based on the power requirements issued at the end of the design loop 0. Their characteristics and design assumptions are quickly resumed in Table 1 and Table 2.

For this loop, the size of the turbomachine is fixed and the consumption map is used in the design process without scaling. On the contrary, the generator's efficiency as well as specific power and power density are considered constant and the components can be resized during the process.

It must be emphasized that the turbomachine design has a PSFC about 20% higher than the component used in the initial design loop. This increase was unexpected and raised the question of how would this higher fidelity component design compare to the turbofan engine considered for the reference aircraft. This last one has not been the object of refined analysis and the comparison may not be on the same level of accuracy. To try to answer this question an efficiency breakdown analysis is later proposed in Section IV.

The generator design was performed for a single generator of 11MW while the architecture considered two generators of 5.5MW mounted in parallel on a single turboshaft. Upon discussion with the partners, the choice of a single generator is justified to reach a high specific power. If two different power-lines are needed it is possible to design a single machine providing two different outputs. With a single generator, from the point of view of the safety and architecture design, the One Generator Inoperative condition is equivalent to One Turboshaft Inoperative. However, according to the disciplinary specialists, the converter is the part with the highest failure rate. Additionally, separated windings in the generator would provide the same redundancy feature as two generators. Therefore, the OGI case remained adequate to characterize failure of a converter or a winding. Hence, no further modifications were done for the sizing of the propulsion architecture. It is however advised to further analyse the impact that this change has on the safety of the architecture and its sizing procedure.

It was agreed with the partners that the specific power of the generator accounting for passive weight is half that

Table 1 Characteristics of the turbomachine designed for the SMR-CON

Dimensions	
Max outer diameter	1.0 m
Length	2.3 m
Nominal power and performances	
Nominal power in TOC	7.95 MW
Power turbine working speeds	6000RPM – 9500RPM
PSFC in TOC	0.164 kg/(kWH)
Weight	1136 kg
Design hypothesis	
Max T41	1900°K
OPR	48
Cooling taken from HPC	20% for HPT, 10% for LPT

Table 2 Characteristics of the generator design for the SMR-CON

Dimensions	
Diameter	0.54 m
Length	0.98 m
Mass	
Specific power (active)	19.3 kW/kg
Power density (active)	49 kW/L
Nominal power and efficiency	
Power (TO)	11MW
Speed	8200 RPM
Efficiency	0.99
Hypothesis	
Typology	PMSM rotor
Convection coefficient	1000 W/(K.m^2)

of the active parts alone. The uncertainty accompanying the estimation of passive weight is then analysed in design exploration.

One may note the important efficiency improvement compared to D1.3 (from 0.95 to 0.99). The efficiency may be slightly different in off-design conditions. This will be treated as an uncertainty and analysed through design exploration.

B. Propulsion units and electric cables

The work package dedicated to Electric Propulsion Unit designed Electric Motors (EM) and Power Electronics (PE) using two different cooling options: the advanced air cooled and the liquid cooled. Their characteristics are briefly described in Table 3. The technique retained for both cooling options is an integrated design where both the EM and PE are packaged in a single component: the Electric Propulsion Unit (EPU). This EPU is then placed inside the fan hub.

Similarly to the genertor, the EPU are resized during the design process considering constant specific power, power density and efficiency.

Table 3   Characteristics of the designed Electric Motor (EM), Power Electronics (PE) and the combined performances of Electric Propulsion Unit (EPU)

	Parameter	EM		PE		EPU	
		Advanced air cooled	Oil cooling	air cooled	liquid cooled	air cooled	liquid cooled
Active parts	Specific power [kW/kg]	12.1	22.7	37.7	37.7	9.1	14.1
	Efficiency (%)	98.71	97.9	98.8	98.8	97.53	96.73
Standalone	Specific power [kW/kg]	7.3	14.8	12.7	24.7	4.6	9.2
	Efficiency (%)	98.71	97.9	98.8	98.8	97.53	96.73
	Length to Diameter (active)	2.1	1.1	-	-	-	-
	Power density kW/L	28.8	60.1	4.4	6.7	3.8	6

The air cooled option was judged to perform too poorly after the first OAD evaluations and the nominal configuration of the SMR-CON was quickly re-oriented toward the liquid cooled option.

The EPU being placed in the efan hub, the diameter of the hub is calculated based on EM power density and length to diameter ratio. The total length of the hub takes into account the PE through the PE power density. Hence, components reaching high power density will be an advantage to reduce the total wet area.

The low power density of the EPU (maximum 6 kW/L), mainly due to the PE, will result in a long hub design, high wet area and aerodynamics penalties. However PE's power density may vary largely from 5kW/L up to 30kW/L, driven mainly by the cold plate design and the cooling strategy and no previous work could help determine the correct order of magnitude. In this study, the low power density is a high penalty and it was chosen to use the previous 20kW/L value for the PE for the nominal SMR-CON performance analysis. The effect of power density is then analysed from design exploration and sensitivities.

It is important to note that the oil cooled solution does not take into account the weight of pumps, heat exchanger or drag penalty due to air intake, this is evaluated separately at the Thermal Management System (TMS) level. The main idea for TMS of the EPU is to dissipate the heat through skin conduction. Taking benefit of the distribution of the propulsion, a large surface area is provided by the nacelle, fans and the wing for heat dissipation. Preliminary analysis (based on the work by Kellermann and al [13]) showed sufficient heat dissipation potential through skin conduction for

liquid temperature of 90°C at the skin level. The TMS is however still to be defined in details.

A cable harness design was provided for cables going from generators to cores and from cores to EPU. Aluminium cables were designed for DC and low power AC transmission lines and copper cables for high power AC. In addition, the additional insulation weight to withstand 3KV has been included in the design. The cables presented in Table 4 are labelled F1 to F4 corresponding to:
- F1: from generator to AC-DC converter,
- F2: from convert to core,
- F3: from core to EPU,
- F4: from Power Electronics to Electric motor.

The cable model implemented in the OAD tool was calibrated to match the data presented here. Specifically, the harness temperature was raised to match the maximum intensity, aluminium cables were added to the possible choice and insulation weight to withstand +-1500V was deduced.

Table 4   Cable designs

ID	Type	Core material	Wire Gauge	Number of phase	Harness details	Number of wire	Linear mass density (kg/m)	Efficiency
F1	AC	Copper	#0000	3	6 wires per phase in star spacer	18	26.8	99.96%
F2	DC	Aluminium	#0000	2	3 wires per phase in star spacer	6	4.8	99.97%
F3	DC	Aluminium	#1	2	2 wires in bundle / 3 bundles	4	1.8	99.94%
F4	PWM	Aluminium	#2	3	4 wires per phase in star spacer	6	2.3	99.96%

A recommended 50% penalty on overall cable weight to account for connectors, jacket, sheaths and accessories was applied.

It has been assumed that the converters and generators are packaged together or closely integrated in the same fashion as the EPU so as to reduce cable weight and filtering components. Therefore, no AC cables are assumed between generators and converters.

A detailed geometric integration of the cables in the airframe was not possible, although insights on the volume occupied by the cables and the separation between harnesses had been provided by the partner. This input led the consortium to see the geometric integration of cables as the next burden to investigate.

Finally, the initial specific power estimate (20kW/kg) is to be conserved for the electric cores.

C. Consideration on Thermal Management System (TMS)

The TMS solutions envisioned for the generator and converter relies on a liquid to air compact heat exchanger. To cover the ground and taxi phases with low dynamic pressure, it is envisioned to use a puller fan drawing current from the generator. The model uses a heat exchanger efficiency defined as[14]:

$$\eta_{ex} = \frac{q}{q_{max}} = \frac{C_{air}\left(T_{air_{out}} - T_{air_{in}}\right)}{C_{min}\left(T_{liq_{in}} - T_{air_{out}}\right)} \tag{1}$$

The power losses to dissipate as heat, P_L, is equal to the heat to dissipate through the heat exchanger q. Additionally, assuming that the minimum heat capacity rate C_{min}, is provided by the air due to its low specific heat compared to liquid coolant, that is $C_{min} = C_{air}$, one may write:

$$P_L = \eta_{ex}q_{max} \tag{2}$$

$$P_L = \eta_{ex}C_{min}\left(T_{liq_{in}} - T_{air_{out}}\right) \tag{3}$$

$$P_L = \eta_{ex}\dot{m}c_{p_{air}}\left(T_{air_{out}} - T_{air_{in}}\right) \tag{4}$$

$$\dot{m} = \frac{P_L}{\eta_{ex}c_{p_{air}}\left(T_{air_{out}} - T_{air_{in}}\right)} \tag{5}$$

In this equation, the baseline value of $\eta_{ex} = 0.4$ and $T_{liq_{in}} = 150^\circ C$ are taken from literature[14] and from the generator's design assumptions respectively. The power penalty is then computed assuming a puller fan:

$$P_{cool} = \dot{m}c_{p_{air}}T_{air_{out}}\left(FPR^{\frac{\gamma-1}{\gamma\eta_{fan}}} - 1\right) \tag{6}$$

Where the Fan Pressure Ratio (FPR) compensates the pressure losses through the heat exchanger, intake and exhaust. Therefore no thrust is expected from this puller fan. The pressure loss is taken from figures of merit provided by one of the partner and is equal to 0.1.

The weight penalty deduced by the partners to account for liquid, tubing, pumps, etc... is identical to the initial estimate of 0.5 kg/kW used in the previous design loop.

IV. Potential of turbo-electric propulsion compared to turbofan

This section will describe the efficiency analysis of the turbo-electric and distributed propulsion and compare it to a turbofan engine. It provides a better understanding of the relative importance of each components of the turbo-electric architecture in the global propulsive efficiency.

A. Efficiency analysis

The overall efficiency of the turboelectric propulsion chain may in the end be compared to a turbofan through the TSFC. However, this does not inform the reader about the trade off between a propulsive efficiency gain and electrical power transmission losses at play in the turboelectric architecture, nor does it allow a detailed comparison or benchmark with a classical turbofan. To put the two propulsion architecture in perspective, a methodology is proposed to decompose the TSFC in all sub-component efficiencies to allow a detailed comparison.

1. TSFC decomposition

The methodology starts by defining the efficiencies used subsequently. Here the definitions adopted by GasTurb [15] are adopted. The TSFC can be written as:

$$TSFC = \frac{V}{\eta_{th}\eta_{p}LHV} , \tag{7}$$

with the thermal efficiency η_{th}, the propulsive efficiency η_p and the kerosene Lower Heating Value, $LHV = 43$MJ/kg. The thermal and propulsive efficiency are expressed physically using the rate of change of the air kinetic energy through the engine as:

$$\eta_{p} = \frac{\text{Propulsive power}}{\text{Rate of change kinetic energy}} \tag{8}$$

$$\eta_{th} = \frac{\text{Rate of change kinetic energy}}{\text{Fuel power}} \tag{9}$$

When multiplying together the propulsive and thermal efficiency, one obtains the overall efficiency of the propulsion. The thermal efficiency can be further decomposed as:

$$\eta_{th} = \eta_{tr}\eta_{core} , \tag{10}$$

where the core efficiency η_{core}, and the transmission efficiency η_{tr}, are expressed as:

$$\eta_{\text{tr}} = \frac{\text{Rate of change kinetic energy}}{\text{Power in flow at core exit}} \tag{11}$$

$$\eta_{\text{core}} = \frac{\text{Power in flow at core exit}}{\text{Fuel power}} \tag{12}$$

The core exit of the turbo-machine is defined here as the station where all the work needed to drive the compressor and compensate intake losses has been taken out of the flow. At the core exit, the power remaining in the flow is what is available to generate propulsive power. For both turbofan and turbo-shaft, we assume that the turbo-machine architecture allows to place this station right before the power turbine which is driving only the fan or the generator. It is obviously not the case for all turbo-machine architecture (especially those having the low pressure turbine driving both the low pressure compressor and the fan) but it simplifies the present analysis.

The definitions given here take different mathematical expression for turbofan or turbo-electric propulsion, but they have the same physical meaning, which is the real interest here. In the two subsequent paragraphs, the efficiencies for turbofan engine and turbo-electric propulsion are described.

2. Turbofan engine

The turbofan engine is represented with two separated flows, the hot flow and the cold flow. The BPR is estimated to be 16 corresponding to an Ultra High By-pass Ratio engine for Entry Into Service 2035. The exhaust velocity ratio between the cold flow and the hot flow is assumed to be 0.5. The fan is modelled as a single stage compressor and is sized to match the thrust requirement considering the imposed BPR, the Fan Pressure Ratio (FPR) and the thrust of the hot flow as shown in Figure 6.

List of assumptions for turbofan engine modelling:
- UHBR type, BPR=16,
- Thrust 23700N @ 35kft, M=0.78,
- FPR=1.45
- $\frac{M_c}{M_h} = 0.5$
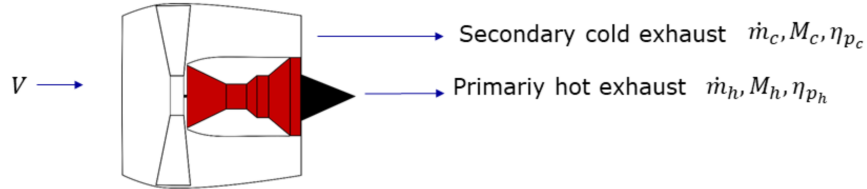
Fig. 6 Turbo-fan engine simplified model

To compute the propulsive efficiency; the propulsive power is deduced from thrust and airspeed as: TV. The rate of change of kinetic energy through the engine is deduced from the exhaust airspeed as: $\frac{1}{2}\dot{m}\left(V_{ex}^2 - V^2\right)$. To deduce the thermal efficiency, the TSFC level of the UHBR engine in cruise conditions, that is $TSFC = 14.5\,g/kNs$, is used. This is summarised in Table 5.

Table 5 Turbofan propulsive and thermal efficiency.

	$\dot{m}$ (kg/s)	Mach	Thrust (N)	$\eta_P = \frac{TV}{0.5\dot{m}\left(V_{ex}^2 - V^2\right)}$	Combined η_P	$\eta_{\text{th}} = \frac{V}{TSFC\,\eta_P\,LHV}$
Cold exhaust	195.5	1.09	18 356	0.84	0.74	0.51
Hot exhaust	12.2	2.24	5 338	0.52		

The combined propulsive efficiency is the result of the propulsive thrust over the total kinetic energy change through

the engine. One key to the exceptionally high propulsive efficiency of turbo-electric propulsion is to get rid of the hot flux.
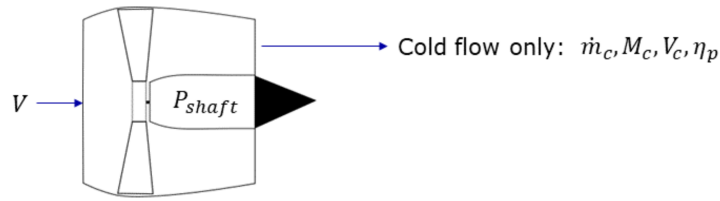
3. Turboelectric propulsion

The electric fan is modelled with the same single stage compressor model as the turbofan (see Figure 7).
List of assumptions for electric fan modelling:
- Thrust 23700N @ 35kft, M=0.78,
- FPR = 1.15,
- Number of fan: 12,
- No thrust from turboshaft.

Using the performance figure of the turbo-machine in cruise conditions, $PSFC = 0.164$ kg/kWH and the global electric power transmission efficiency of $\eta_e = 0.93$, the propulsive and thermal efficiency of the turbo-electric propulsion may be calculated. The results are summarised in Table 6.

Fig. 7   Simplified electric fan model.

Table 6   Turbo-electric propulsive and thermal efficiency. The fuel flow is scaled for one e-fan.

	$\dot{m}$ (kg/s)	Mach	Thrust (N)	$\eta_p = \frac{TV}{0.5\dot{m}(V_{ex}^2 - V^2)}$	$\dot{m}_f = \frac{P_{shaft}}{\eta_e} PSFC$	$\eta_{th} = \frac{V}{TSFC\,\eta_p\,LHV}$
Cold exhaust	53.5	0.90	1975	0.93	99.4kg/h	0.42

Thanks to the absence of thrust from a hot exhaust and a large BPR, the propulsive efficiency of the DEP is higher than the UHBR engine (0.93 versus 0.74) but its thermal efficiency is lower (0.42 versus 0.51) because it accounts for the losses in the electric power transmission system. The motivation for turbo-electric propulsion being that the higher propulsive efficiency should compensate for the lower thermal efficiency and provide a global efficiency gain. The electric losses being hidden behind the thermal efficiency for the turbo-electric, it is necessary to decompose the thermal efficiency to have a complete picture.

Figure 8 shows the turbo-electric chain efficiency breakdown. Using the definition of the transmission efficiency (11), η_{tr} can be computed from the electrical power transmission efficiency, the power turbine efficiency η_{PT} and the electric fan efficiency as:

$$\eta_{tr} = \eta_{PT}\eta_e\eta_{fan} \tag{13}$$

with the fan efficiency defined as the rate of change of kinetic energy through the engine over the electric motor shaft power.

For the turbofan engine, the transmission efficiency was estimated by considering the fan efficiency and the efficiency of the power turbine for the cold exhaust and negligible duct losses for the hot exhaust. This gave an estimated $\eta_{tr} = 0.85$ which aligns with what could be found in the literature [16] especially when considering EIS 2035.

The complete picture and comparison between turbofan and turbo-electric propulsion is given in Table 7. In this analysis, the power turbine efficiency was assumed equal for both propulsion and the fan efficiency is found to be similar. The transmission efficiency of the turbo-electric propulsion is penalized by the electrical efficiency although, thanks to the good propulsion efficiency, the global efficiency of the turbo-electric propulsion is higher. On the point of view of propulsion engineer, the goal is reached since the propulsive efficiency compensates for the electric power losses and provides a small overall advantage.
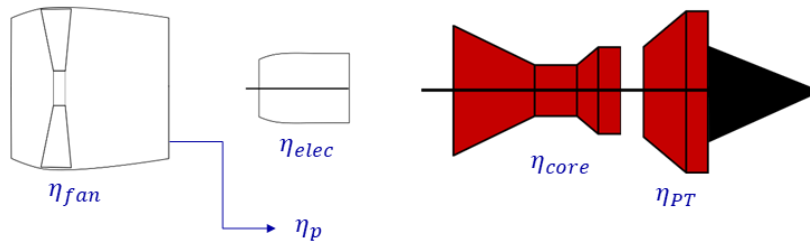
Fig. 8   Turbo-electric efficiency breakdown.

However this advantage is small, and one can doubt that the weight and drag penalty of the turbo-electric propulsion could be compensated by the better fuel efficiency. The reason for such a small advantage may be found in the lower turbo-electric core efficiency. A turbofan and a turbo-shaft may share the same hot core so no significant difference should be noticeable in the core efficiency. When calculating the hot core efficiency of the turbo-machine from the detailed thermodynamic model, the value of 0.57 was confirmed. Further optimization of the turbo-machine failed to increase the core efficiency, especially after taking into account the intake losses arising from the integration of the generators in front of the turbo-machine. A detailed thermodynamic model of the reference turbofan, to confirm the turbofan core efficiency was not available in the project. Overall the thermal efficiency decomposition of the turbofan engine is a limitation of this work. Improving the analysis on this point would indicate if the turbo-electric propulsion really holds a disadvantage in terms of core efficiency or if it could be equal or greater than a turbofan. In which case, the turbo-electric propulsion would confirm its advantage in term of propulsive efficiency.

Table 7   Efficiency breakdown. The transmission efficiency of the turbofan takes into account the hot exhaust.

	η_{core}	η_{PT}	η_e	η_{fan}	η_{tr}	η_p	η_{th}	η_{global}
Turbofan	0.60	0.91	-	0.875	0.85	0.74	0.51	0.377
Turbo-electric	0.57	0.91	0.93	0.88	0.74	0.93	0.42	0.39

V. Results

The SMR-CON aircraft is evaluated and compared against a baseline aircraft (BAS). This aircraft is a projection for Entry Into Service (EIS) 2035 of a traditional tube and wing aircraft equipped with conventional kerosene UHBR engine. The assumptions used to operate the projection to EIS2035, especially the specific fuel consumption, are first discussed in the following subsection.

Both the BAS and the SMR-CON aircraft are sized for the design mission of 2750NM. They are then evaluated based on a typical mission of 800NM with the design payload. The TLARs are available Table 17 in annex.

A. Technology assumptions for EIS 2035

The technology assumption for EIS2035 are applied to both the BAS and SMR-CON aircraft with a few differences when applicable (see Table 18 in annex).

The SMR-CON aircraft keeps a 5% penalty on the overall friction drag coefficient (CD0) to account for the integration of the DEP. No aerodynamics evaluations were planned for SMR-CON within the scope of IMOTHEP. This penalty was therefore not discussed and is inherited from the DRAGON concept.

B. Performances compared to REF and BAS

The SMR-CON is evaluated in its nominal version (oil cooled EPU) against the BAS aircraft. The main performance figures are compared in Table 8.

In the nominal configuration, the SMR-CON has a fuel burn in operational mission 2.1% higher than the BAS

Table 8   SMR-CON aircraft performances compared to BAS aircraft

Parameters	BAS	SMR-CON D15	SMR-CON wrt BAS (%)
MTOW (kg)	69802	76789	10
OWE (kg)	40053	45472	13.5
Propulsion weight(kg)	8370	12897	54.1
L/D max	18	17.1	-5.1
Fuel burn (sizing mission)(kg)	11700	12869	10
Reserve (sizing mission) (kg)	2468	2931	18.8
Fuel burn (typical mission)(kg)	3828	3908	2.1
Reserve (typical mission) (kg)	2231	2692	20.7
TSFC (g/kNs)	14.5	13.4	-7.5
AR	10.9	10.9	0
Span (m)	34.4	35.6	3.4
Wing area (m^2)	108	115.9	6.9

aircraft. Despite the better TSFC, the penalties brought by the turbo-electric propulsion, +5T in OWE and -5% in L/D, are too important to reduce the final fuel burn.

An additional remark concerns the reserve fuel of the BAS aircraft. A notable difference in engine efficiency could be observed during the holding phase at low altitude, speed and power level. The holding phase alone is responsible of 400kg difference in fuel burn, which led to question the engine model used for the BAS aircraft. Upon verification, during the holding phase, the engine model of the BAS is working outside of its interval of confidence (due to low thrust level), hence the value are extrapolated and may be largely optimistic. On the contrary the tabulated data of the turboshaft are covering well this region. Hence, the fuel burn obtained for the holding phase for the SMR-CON can be regarded as more realistic results.

The details of the turbo-electric propulsion chain of the SMR-CON in the nominal configuration is given in Table 9. Please note that here the EM and PE specific power take into account the weight penalty for cooling. Additionally, the cooling system power output refers to the maximum heat flux that the TMS has to dissipate per turbo-generator.

The components of the propulsion system are all sized by the Take-Off Field Length requirement except for the fan geometry (sized for cruise) and the turbomachine (not resized during the OAD process). Since the takeoff phase is very short (40s), it would be of interest to overload some of the electrical component so as to downsize the propulsion system and save weight.

The heat losses per component and in different flight conditions are given in Table 10.

The maximum losses are encountered during takeoff. Shortly after take off the power level may be reduced to match a specific climb profile. For the sizing mission, the power level is maintained to the maximum to reach the time to climb (<25min). In both situations, this high power level is transitory and the steady state regime in cruise is much less demanding. One may take advantage of the transient part here again to avoid oversizing the TMS.

C. Design Sensibilities

Parametric explorations are used for two purposes:
- Explore the effect of varying the sizing mission,
- Identify a set of components characteristics that would allow advantageous performances compared to BAS,

For each goals a separate parametric exploration, with a dedicated design of experiment is done. These analyses are presented and commented in the following subsections.

Table 9   Components of the propulsive chain (characteristic of single component)

Components	Number of component	Maximum output Power (MW)	Efficiency	Specific power (kW/kg)	Masses (for one element) (kg)
Turboshaft	2	7.95	-	7	1136
Generator	4	5.468	0.99	10	547
Converter	4	5.358	0.98	19	282
Cable before core (AWG 4/0) aluminium	64	3000V, 304 A	1	0.8 kg/m + 50%	1184
Core	4	5.272	0.99	20	264
Cable after core (AWG 0/1) aluminium	4	3000V, 163 A	1	0.45 kg/m + 50%	626
Power Electronics	24	0.868	0.988	19	45.7
Emotor	24	0.85	0.979	11.2	75.7
Fan and gearbox assembly	24	-	1	27.4	31
Generator and converter TMS	2	0.329	1	2 kW/kg	325

Table 10   Power and heat loss of each components of the propulsion chain (single component)

| Component	Maximum output power (kW)	Efficiency	Losses at take off (kW)	Losses at TOC (kW)	Losses at cruise (kW)
Emotor	850	0.979	18.2	14.4	10.2
Inverter	868	0.988	10.5	8.4	6
Core	5272	0.99	53.3	42.2	29
Converter	5358	0.98	111.6	85.7	58.5
Generator	5468	0.99	55.2	43.7	29.9

1. Sizing mission parameters

It was of interest to investigate if a design mission with a shorter range could be advantageous to the SMR-CON aircraft. The effect of the design range, the number of passenger and the cruise Mach number were varied to also estimate the variations of performance when the concept is extended into a family of aircraft. The domain of variation of the mission parameters is presented in Table 11.

Table 11   Mission variables and bounds for sensitivity analysis

Parameter	Nominal	Min	Max
Pax	150	120	200
Range (NM)	2750	1200	3100
Mach	0.78	0.78	0.82

A Design Of Experiment consisting of 40 aircraft sampled via Latine Hypercube Sampling method [17] was calculated, the resulting configuration are evaluated on the typical mission range (800NM) plotted on 2d graphics in Fig 9. As the number of passenger is a varying parameter, the fuel burn per pax is presented to allow a better evaluation of aircraft performances. It is clear that the number of pax has a large influence on the final fuel burn and the fuel burn per pax. For the design range the observable trend tends to confirm the hypothesis; the aircraft efficiency does improve with reduced design range. Finally, the cruise Mach number has a low impact compared to the two other variables.
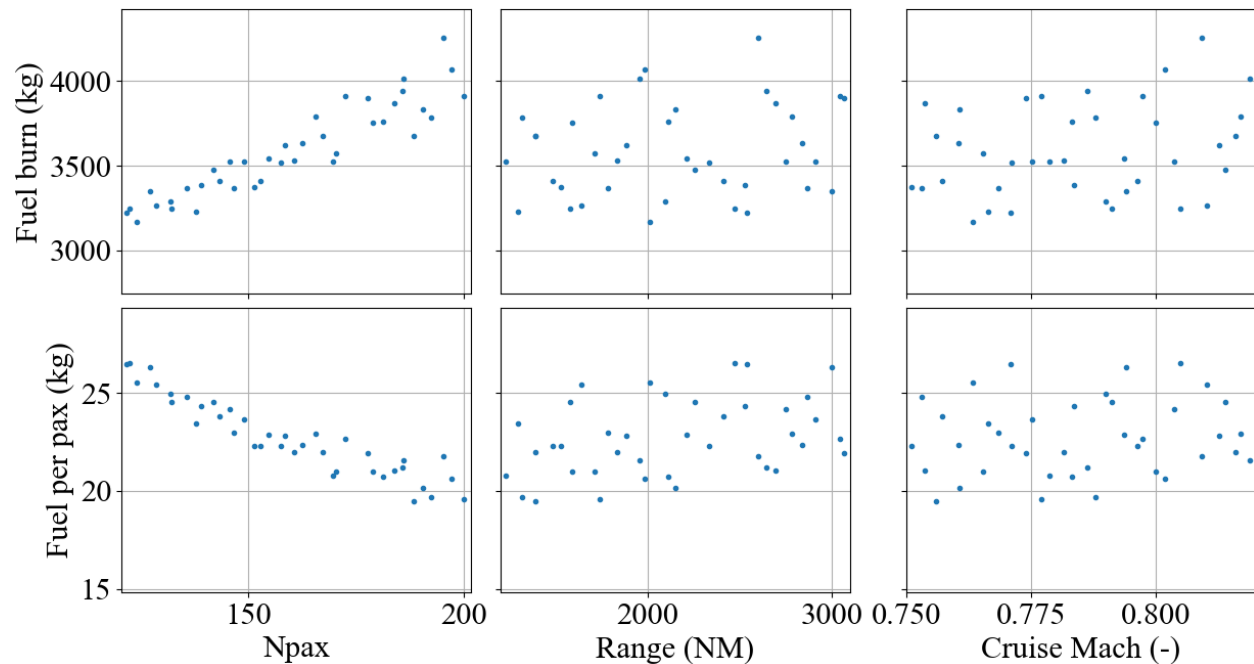
Fig. 9   Influence of design mission parameters on the SMR-CON fuel burn

As reducing the design range was shown to have a beneficial effect, an evaluation against the BAS aircraft with a reduced design range was pursued. Table 12 shows the comparison between the BAS & SMR-CON aircraft sized with a design range of 1200NM.

Important improvements are visible for the SMR-CON in terms of weight. The MTOW and OWE come very close to the BAS aircraft and the overall fuel burn is improved such that the SMR-CON consumes 1.5% less fuel than the BAS during the operational mission.

Reducing the range of the design mission does improve the fuel burn of the SMR-CON and could be used together with other design parameters, explored in the next sections, to improve the overall performances of the SMR-CON aircraft.

Table 12   Performance evaluation of SMR-CON and BAS aircraft for a reduced design mission.

Parameters	BAS (1200NM)	SMR-CON (1200NM)	SMR-CON wrt BAS (%)
MTOW (kg)	61738	63428	2.7
OWE (kg)	38732	39672	2.4
Propulsion weight(kg)	8364	9978	19.3
L/D max	17.9	16.9	-5.8
Fuel burn (sizing mission)(kg)	5192	5593	7.7
Reserve (sizing mission) (kg)	2234	2639	18.1
Fuel burn (operational mission)(kg)	3769	3712	-1.5
Reserve (operational mission) (kg)	2193	2609	18.9
TSFC (g/kNs)	14.5	13.7	-5.5
AR	10.9	10.9	0
Span (m)	33.6	34	-0.2
Wing area (m^2)	106	106	-0.4

2. Sensitivity to turbo-electric components characteristics

By turbo-electric components, it is referred to EPU, power generation and power transmission. Only the cores are omitted from this parametric exploration as they were not the subject of a design exercise. Since power generation and propulsion unit always include an electric machine and power electronics, both systems will be treated as integrated assembly for the parametric exploration so as to reduce the number of variables. It will be referred to the EPU specific power as being the specific power of the combined electric motor and power electronics. The combined value of specific power for the EPU is obtained by the following equation:

$$P_{S_{EPU}} = \frac{1}{\frac{1}{P_{S_{EM}}} + \frac{1}{P_{S_{PE}}}}$$

(14)

Similarly for power generation, the specific power refers to combined generator and converter specific powers. The same applies for efficiency and power density.

The input parameters and the range of variation selected for the parametric study are shown in Table 13.

The range of variation for this study follows the recommendations received from the different partners, essentially considering that the nominal characteristics are conservative. For the EPU, the range of variation covers advanced air cooled technology to oil cooled technology with additional 50% improvement in specific weight and power density. For power generation, it is assumed up to 50% improvement in specific power of both generator and converter (baseline for converter is 20kW/kg). Few indications were available for the power density so it was decided to re-use the EPU values but knowing that the current generator design is less dense than electric motor.

The lowest bound for efficiencies are based on lowest estimates from WP and upper bounds is defined to allow exploration. For power transmission the voltage was varied from 1kV to 3kV. The voltage recommended for the SMR-CON aircraft, which explore a so called conservative configuration, was initially 1kV. This voltage level was found to be very penalizing for the integration of the cables in the structure and the weight. It was obvious from the first OAD evaluation that a 3kV voltage level was enabling the configuration although very challenging on the point of view of partial discharges and initially reserved for the more radical configuration (the SMR-RAD).

The turboshaft performance level was varied from +4% to -15% which covers the different performance evaluation given during the initial and current design loop.

Table 13 Propulsive components variables and bounds for the sensitivity analysis.

Component	Characteristic	Nominal	Min	Max	Label
EPU (Electric motor + inverter)	Specific Power (kW/kg)	9.2	4.6	15	a)
	Power density (kW/L)	15	3.8	20	b)
	Efficiency	0.967	0.96	0.99	c)
Power generation (Generator + converter)	Specific power (kW/kg)	6.55	6	10	d)
	Power density (kW/L)	11	3.8	15	e)
	Efficiency	0.97	0.96	0.99	f)
Turboshaft	PSFC (kg/kNs)	0.164	0.145	0.17	
	Multiplier	1	0.885	1.04	g)
Power transmission	Voltage (V)	3000	1000	3000	h)

A DoE of 200 points sampled with Latine Hypercube Sampling, ensuring a coverage of the whole interval of variation, has been generated. For each set of input a new aircraft is calculated by the OAD tool, keeping all other input equal to the version presented in Table 8. The 2d graphical representation of the resulting aircraft are shown in Fig 10.
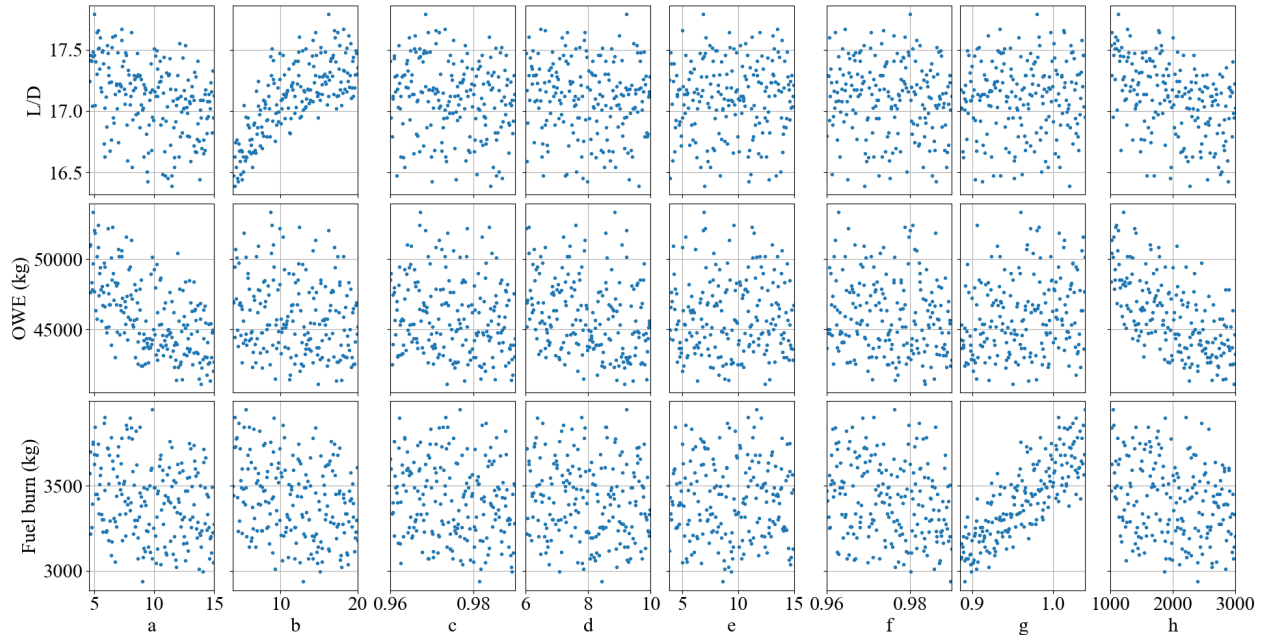
Fig. 10 SMR-CON performance sensitivity to propulsive components characteristics (see Table 13 for labels). Here fuel burn doesn't include taxi and take-off phases. The equivalent fuel burn of the BAS aircraft is 3480kg.

From Fig 10, it is obvious that the variation of PSFC (label 'g') is influencing the most the fuel burn. The lift to drag ratio illustrates well the coupling between EPU power density and the length of the efan hub (b). A non-linear behaviour can be seen, where a power density lower than 15kW/L affects highly the L/D ratio. Additionally, the voltage level (h) and the EPU's specific power (a) are shown to have a notable influence on L/D, OWE and fuel burn. Noticeably, the L/D reduces when the voltage or the specific power increases. This is because a heavier aircraft has larger wing surface

area and wingspan, which in turn offer better drag characteristics. However, some of these heavy configurations may not comply with the 36m wingspan limit and their aspect ratio eventually would have to be reduced. This sensitivity should therefore be taken with care.

The remaining clouds have an important dispersion making it difficult to guess the main tendencies.

Out of these data points, it was of interest to identify and extract typical configurations ensuring different level of fuel reduction compared to BAS aircraft and give the corresponding propulsive components characteristics. This has been done in Table 14.

Table 14   Typical configurations and associated components characteristics to reach different performance levels with respect to BAS.

	Configuration number	N0	N1	N2	N3
Results	**Fuel burn wrt BAS**	0% (3480kg)	-5% (3306kg)	-10% (3132kg)	-15% (2980kg)
	L/D	16.9	16.9	17	16.8
	OWE (T)	44.5	43.5	44	42.5
Input parameters	**Turboshaft PSFC**	-1%	-2% to -5%	-7% minimum	-11%
	EPU				
	Specific power (kW/kg)	11	>11	6.5	9
	Power density (kW/L)	15	>17	18	13
	Efficiency	0.97	>0.975	0.988	0.982
	Power generation				
	Specific power (kW/kg)	8	>8	8.4	8.4
	Power density (kW/L)	Indifferent	Indifferent	12	9
	Efficiency	0.97	>0.975	0.985	0.99
	Voltage (V)	>2100	2600	2300	2300

The main lever of action is the turboshaft PSFC; to ensure an interesting 10% fuel burn reduction compared to BAS, no less than 7% PSFC reduction could be found in the DoE. For the particular combination shown in the table, the additional 3% is brought by good electrical efficiencies (>0.985%) and rather high power densities to reduce wet surface area and achieve a good L/D, despite the rather low specific powers. This is only one example, but trading electrical efficiency for better specific powers may also lead to similar results.

Generally, a good performance level can be achieved by increasing electric component efficiencies and power density (up to values around 10-12kW/L for the EPU) together with a reduction of the PSFC (going from configuration 0 to configuration 2). Then the ultimate lever of action is to increase the specific power (configuration 3). It can be noted that the best configuration (3) is still relatively far from the boundaries for specific power and power density in comparison with efficiencies. In opposition, configuration 0 shows higher specific power and power density that compensate for low efficiencies but with less impact on the fuel burn.

Of course these configurations are only typical and the level of performance can be achieved by trading one characteristic with another.

Sensitivity evaluation with fixed PSFC.

The previous DoE showed the importance of the turbomachine performance over the electric component characteristics. As such, this analysis brings little information on the level of performance that the electric components must have to ensure a significant advantage over the BAS aircraft. Similarly, it is difficult to conclude on the direction of research and set milestones for the electrical components.

Therefore, it was decided to repeat the sensitivity analysis with a fixed PSFC and a 10% improvement leading to typical in cruise PSFC=0.148kg/kNs. With a fixed PSFC, only the performances of the electric components will be investigated to identify the key enablers for major fuel burn reduction compared to BAS.

Since the sensitivity depends on the range of variation of the input parameters and in order to do a fair comparison between the parameters, the range of variation of specific power, power density and efficiency have been harmonized for this particular DoE (see Table 15).

The 2d plots of the 200 points DoE corresponding to Table 22 are shown in Fig 11.

Table 15   Propulsive components variables and bounds for the sensitivity analysis with fixed PSFC.

| Component	Characteristic	Nominal	Min	Max	Label
EPU (Electric motor + inverter)	Specific Power (kW/kg)	9.2	5	15	a)
	Power density (kW/L)	15	3.8	20	b)
	Efficiency	0.967	0.96	0.99	c)
Power generation (Generator + converter)	Specific power (kW/kg)	6.55	5	15	d)
	Power density (kW/L)	11	3.8	20	e)
	Efficiency	0.97	0.96	0.99	f)
Power transmission	Voltage (V)	3000	1000	3000	g)
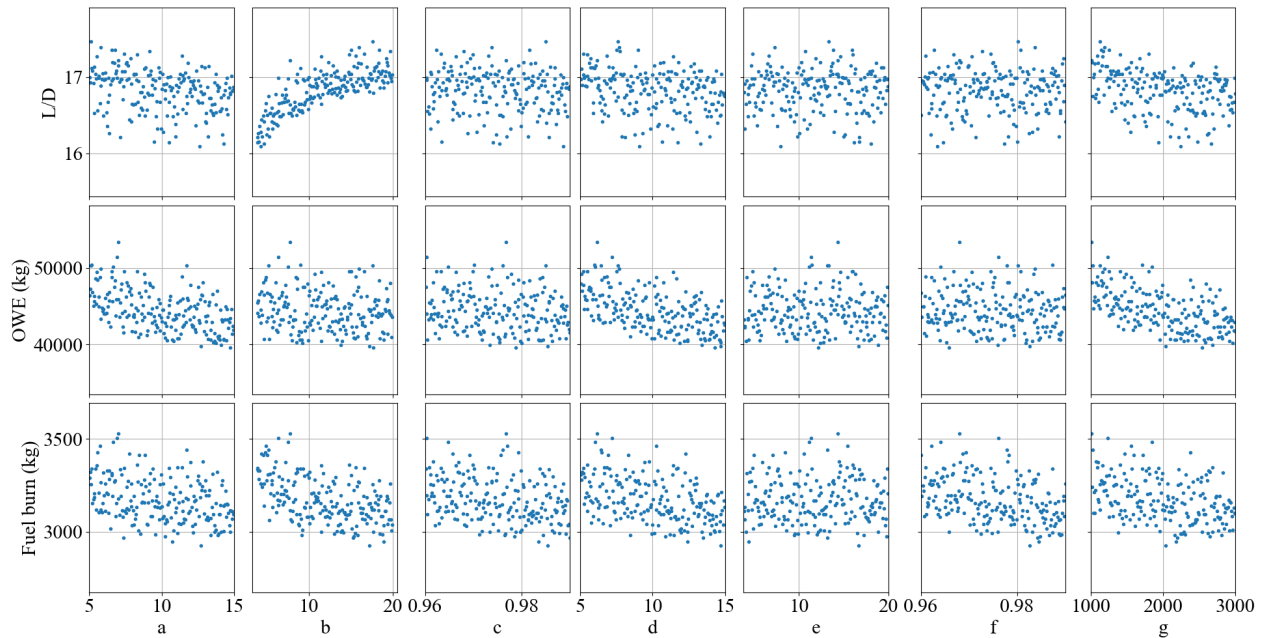
Fig. 11   SMR-CON performance sensitivity to propulsive components characteristics with fixed PSFC (see Table 15 for labels).

Focusing first on the L/D ratio, it is quite clear that the power density of the EPU (label 'a') has the most important impact. On the contrary, the power density of power generation (label 'e') has no impact (later confirmed by the Sobol indices). This may come from the fact that the space allocated to the EPU is constrained by the design of the electric fan. These ones are sized by the target FPR and the number of fans. By reducing the fan number, larger hub diameter would be obtained, offering more volume for the EPU and eventually reducing this impact. On the contrary, the nacelle of the power generation system has a diameter of more than one meter which seems to offer sufficient volume to fit both the generator and the converter with limited impact on the L/D.

The specific powers and the cable voltage reduce the OWE and lift to drag ratio as it was previously observed. Additionally, a non-linear behaviour as a function of the voltage level can be guessed. An optimum could be observed and going to 3kV or high specific power may not be necessary to achieve good performance levels. However, one has to remember that heavy configurations will be limited by the 36m wingspan constraint so this observation cannot be generalized. It can however be regarded as a mean to limit the voltage level below 3kV with limited impacts on the aircraft performances. Further evaluations and coupling effects should be integrated to refine the weight penalty of cable harnesses as a function of the voltage level and confirm the observed tendency.

Finally, all parameters but the power density of power generation affect the fuel burn. To quantify their relative importance, the Sobol Indices[18] have been calculated based on the 200 DoE points using polynomial chaos expansion[19] and represented in Fig 12.
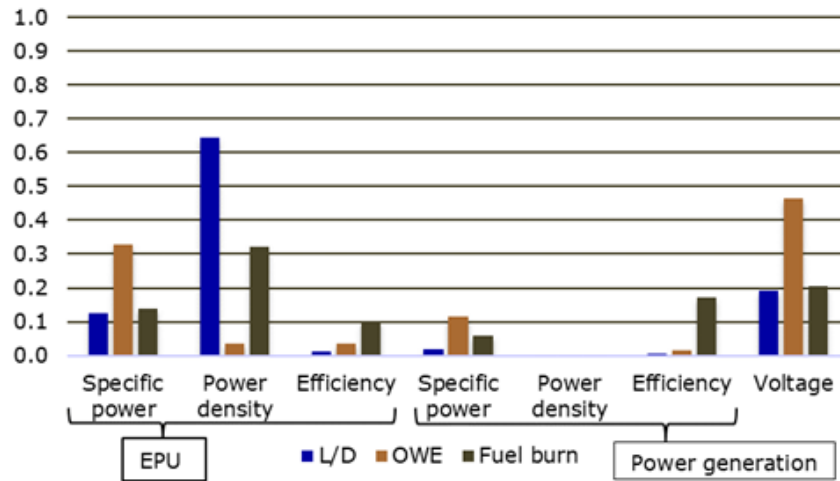
Fig. 12   First order Sobol index

The Sobol Indices could be accurately estimated from the 200 points DoE with very little coupling between input variables (sum of first order index higher than 0.99). Concerning the fuel burn, they show that the EPU's power density is the highest source of variability, second comes the voltage and third the power generation efficiency. Together with the 2D plots, it may be stated that it is critical to improve the EPU's power density to values higher than 10kW/L and voltage to values higher than 2kV, in order to reduce the variability in the aircraft performances and ensure a good performance level. The higher importance of power generation efficiency, over EPU efficiency may be explained by the TMS power penalty being inversely proportional to the efficiency of power generation. While the EPU's efficiency has more effect on the OWE, here again due to the nature of the TMS (see section 2.1.3).

Once again, it is stressed that the important contribution of the EPU's power density to the variation of performances may be mitigated by allowing more volume in the fan hub for reduced wetted surface area. This means increasing the diameter and mechanically reducing the number of fans.

Using the same DoE, a typical configuration allowing 15% fuel burn reduction in comparison with the BAS aircraft is extracted and shown in Table 16.

The example allowing a 15% fuel burn reduction in Table 16 is consistent with the best configuration in Table 14. Both allow important fuel burn savings although the input parameters remain at a certain distance of the upper variation bounds. Under the limitations of the present analysis (especially the number of couplings that are modelled at OAD levels), the components characteristics displayed for these configurations may be taken as milestones. In this sense, a

Table 16   Exemple of a configuration ensuring 15% FB reduction assuming typical cruise PSFC = 0.148 kg/KNs

	Fuel burn wrt BAS	Actual	2975kg, -15%	Difference (%)
Results	**L/D**	17.1	16.8	-1.8
	OWE (T)	45.5	41	-9.9
Input parameters	**EPU**			
	Specific power (kW/kg)	9.2	10.5	14.1
	Power density (kW/L)	15	15.5	3.3
	Efficiency	0.967	0.979	1.2
	Power generation			
	Specific power (kW/kg)	6.55	11	40.5
	Power density (kW/L)	11	20	45
	Efficiency	0.97	0.985	1.5
	Voltage (V)	3000	2650	-11.7

comparison with the current performances is given to evaluate the technology gap. It can be seen that essentially the specific power is the largest relative improvement to be made. Although, even a small increase in efficiency may be more difficult to realise than an increase in specific power. It must be remembered that the power density of the EPU does not exceed 6kW/L and it was replaced by 15kW/L (assuming power density of 20kW/L for the power electronics) for the present analysis. This means that a significant improvement also has to be done in the packaging of power electronics.

Finally, a voltage level of at least 2.5kV has been shown to be necessary to ensure good performances. A lower voltage may be compensated for by other improvements. However a detailed integration of cable harnesses in the aircraft still has to be done to better estimate the impact of power transmission lines. In turn, this should limit the minimum usable voltage due to space or volume limitations.

VI. Conclusion

Within the IMOTHEP project, the preliminary design activities for the SMR-CONservative aircraft consisted in:
- Integration of the designed propulsion components and specifically:
    - The Electric Propulsion Units' figures were updated and a geometrical coupling between fan hub and integrated EPU design was integration in the Overall Aircraft Design process; the cable model was calibrated and new coefficients applied to account for the insulation weight necessary for 3kV; original figures for cores were confirmed.
    - The performance map of a new turboshaft was integrated in the analysis and generator figures were updated considering a single machine and two power outputs. Difficulties were raised to benchmark the turboshaft in comparison with BAS turbofan engine and a methodology to compare the two propulsion system at preliminary design level was proposed.
    - Considerations and figures of merit for the TMS allowed selecting a preliminary solution for the EPU and power generation. The solutions were integrated in the OAD analysis and evaluated at OAD level.
- The SMR-CON performances at the end of DL1 were evaluated and the design sensitivities were explored.

The analysis of the SMR-CON performance at the end of DL1 shows a 2% fuel burn increase compared to the BAS aircraft for the typical mission despite a better propulsive efficiency in cruise. The weight and aerodynamic penalties of turbo-electric propulsion can be designated as main responsible for this level of performance. However, it is not entirely clear how the turboshaft compares with respect to the BAS turbofan in terms of core efficiency. Additional gains may be found in this direction. The sensitivity analysis at OAD level revealed the relative importance of electric components and turbomachine in the performance of the SMR-CON. Although the turbomachine remains a critical component, two typical configurations were identified and can be used as example to define objectives for the electrical components. These configurations assume at least a 10% PSFC reduction and target a fuel burn reduction of 15% with respect to BAS. The results and design choices made during design loop 1 lead to reconsider the number of fans for the SMR-CON. A lower number of fan may be advantageous to offer more volume for the EPU.The integration of electrical cables in the

air frame remains a limitation that could not be studied in details during this first design loop. Further studies on this problematic are planned in the Design Loop 2 of IMOTHEP. Direction of research to improve the SMR-CON outside of the turbo-electric propulsion components include lower design mission range and further aerodynamic studies to remove the 5% friction drag penalty currently considered for the SMR-CON.

Acknowledgments

VII. Nomenclature

SMR	=	Small and Medium Range
CON	=	Conservative
BAS	=	Baseline aircraft for EIS 2035
EM	=	Electric Motor
PE	=	Power electronics
EPU	=	Electric Propulsion Unit
EIS	=	Entry Into Service
TSFC	=	Thrust Specific Fuel Consumption kg/(kNs)
PSFC	=	Power Specific Fuel Consumption kg/(kWH)
L/D	=	Lift to drag ratio
TOC	=	Top Of Climb
TOFL	=	Take Off Field Length
OWE	=	Operational Weight Empty
MTOW	=	Maximum Take Off Weight
AR	=	Aspect ratio
BPR	=	By-pass ratio
UHBR	=	Ultra High By-pass Ratio
P_s	=	Specific Power kW/kg

Appendix

Table 17   TLARs considered for the SMR aircraft in the IMOTHEP project

Parameter	Value
Range	2750 NM
Design payload	15900 kg (150pax @ 106kg/pax)
Cruise Mach number	0.78
Wing span limit	36 m
TOFL (ISA +15, sea level)	< 2200 m

References

[1] Novelli, P., "IMOTHEP* European project : an investigation of hybrid electric propulsion for commercial aircraft," *AIAA AVIATION 2023 Forum*, American Institute of Aeronautics and Astronautics, ???? https://doi.org/10.2514/6.2023-4131, URL https://arc.aiaa.org/doi/10.2514/6.2023-4131.

[2] Atanasov, G., "Plug-In Hybrid-Electric Regional Aircraft Concept for IMOTHEP," , ???? URL https://elib.dlr.de/193104/.

Table 18 EIS 2035 technology assumptions

Aircraft Component	Applied to BAS	SMR-CON
Turbofan / turboshaft engine	SFC -7.0% wrt NEO T/W +3,7% wrt NEO Wetted area to be adjusted	Used turbomachine group inputs instead. Wet area calculated based on geometrical input.
Wing	Mass -10% wrt 2014	Applied
Fuselage	Mass -5% wrt 2014	Applied
Landing gear	Mass -15% wrt 2014	Applied
Pylons	Mass -5% wrt 2014	Applied
Furnitures (seats, galleys, catering,...)	Mass -25% wrt 2014	Applied
Aerodynamics	+3.3% on L/D -5% on CD0 wing -50% on CD wave -10% on CD induced (all wrt 2014).	Additional penalty: +5% on total Cd0 to account for DEP.

[3] Lammen, W. F., and Vankan, W. J., "Conceptual Design of a blended wing body aircraft with distributed electric propulsion," , ???? URL https://hdl.handle.net/10921/1592.

[4] Nguyen, E., Defoort, S., Ridel, M., Donjat, D., Viguier, C., Ali, M., Youssef, T., Gerada, D., and Gerada, C., "Design and performance evaluation of a full turboelectric distributed electric propulsion aircraft: Preliminary results of EU project IMOTHEP," *9th European Conference for Aeronautics and Space Sciences (EUCASS)*, Lille, France, 2022. https://doi.org/10.13009/EUCASS2022-6134, URL https://hal.archives-ouvertes.fr/hal-03810292.

[5] Epstein, A. H., "Aeropropulsion for Commercial Aviation in the Twenty-First Century and Research Directions Needed," *AIAA Journal*, Vol. 52, No. 5, 2014, pp. 901–911. https://doi.org/10.2514/1.J052713, URL https://arc.aiaa.org/doi/10.2514/1.J052713, publisher: American Institute of Aeronautics and Astronautics.

[6] Schmollgruber, P., Atinault, O., Cafarelli, I., Döll, C., François, C., Hermetz, J., Liaboeuf, R., Paluch, B., and Ridel, M., "Multidisciplinary Exploration of DRAGON: an ONERA Hybrid Electric Distributed Propulsion Concept," *AIAA Scitech 2019 Forum*, American Institute of Aeronautics and Astronautics, San Diego, California, 2019. https://doi.org/10.2514/6.2019-1585, URL https://arc.aiaa.org/doi/10.2514/6.2019-1585.

[7] Schmollgruber, P., Donjat, D., Ridel, M., Cafarelli, I., Atinault, O., François, C., and Paluch, B., "Multidisciplinary Design and performance of the ONERA Hybrid Electric Distributed Propulsion concept (DRAGON)," *AIAA Scitech 2020 Forum*, American Institute of Aeronautics and Astronautics, Orlando, FL, 2020. https://doi.org/10.2514/6.2020-0501, URL https://arc.aiaa.org/doi/10.2514/6.2020-0501.

[8] Ridel, M., Nguyen Van, E., Prosvirnova, T., Donjat, D., Seguin, C., and Choy, P., "DRAGON: hybrid electrical architecture for distributed fans propulsion," *MEA 2021*, Bordeaux, France, 2021. URL https://hal.archives-ouvertes.fr/hal-03420612.

[9] Saves, P., Nguyen Van, E., Bartoli, N., Lefebvre, T., David, C., Defoort, S., Diouane, Y., and Morlier, J., "Bayesian optimization for mixed variables using an adaptive dimension reduction process: applications to aircraft design," *AIAA SciTech 2022*, San Diego, United States, 2022. https://doi.org/10.2514/6.2022-0082, URL https://hal.archives-ouvertes.fr/hal-03514915.

[10] David, C., Delbecq, S., Defoort, S., Schmollgruber, P., Benard, E., and Pommier-Budinger, V., "From FAST to FAST-OAD: An open source framework for rapid Overall Aircraft Design," *IOP Conference Series: Materials Science and Engineering*, Vol. 1024, 2021, p. 012062. https://doi.org/10.1088/1757-899X/1024/1/012062, URL https://iopscience.iop.org/article/10.1088/1757-899X/1024/1/012062.

[11] Gray, J. S., Hwang, J. T., Martins, J. R. R. A., Moore, K. T., and Naylor, B. A., "OpenMDAO: An open-source framework for multidisciplinary design, analysis, and optimization," *Structural and Multidisciplinary Optimization*, Vol. 59, No. 4, 2019, pp. 1075–1104. https://doi.org/10.1007/s00158-019-02211-z.

[12] Hermetz, J., Ridel, M., and Doll, C., "Distributed electric propulsion for small business aircraft a concept-plane for key-technologies investigations." DAEJEON, South Korea, 2016, p. 11. Number : hal-01408988.

[13] Kellermann, H., Lüdemann, M., Pohl, M., and Hornung, M., "Design and Optimization of Ram Air–Based Thermal Management Systems for Hybrid-Electric Aircraft," *Aerospace*, Vol. 8, No. 1, 2021, p. 3. https://doi.org/10.3390/aerospace8010003, URL https://www.mdpi.com/2226-4310/8/1/3, number: 1 Publisher: Multidisciplinary Digital Publishing Institute.

[14] Bergman, T. L., and Incropera, F. P. (eds.), *Fundamentals of heat and mass transfer*, 7th ed., Wiley, Hoboken, NJ, 2011.

[15] GmbH, G., "GasTurb 13, Design and Off-Design Performance of Gas Turbines," , 2018. URL https://www.gasturb.de/Downloads/Manuals/GasTurb13.pdf.

[16] Gladin, J. C., Trawick, D., Mavris, D. N., Armstrong, M. J., Bevis, D., and Klein, K., "Fundamentals of Parallel Hybrid Turbofan Mission Analysis with Application to the Electrically Variable Engine," *2018 AIAA/IEEE Electric Aircraft Technologies Symposium*, American Institute of Aeronautics and Astronautics, 2018-07-09. https://doi.org/10.2514/6.2018-5024, URL https://arc.aiaa.org/doi/10.2514/6.2018-5024.

[17] Sacks, J., Welch, W. J., Mitchell, T. J., and Wynn, H. P., "Design and analysis of computer experiments," *Statistical science*, Vol. 4, No. 4, 1989, pp. 409–423. Publisher: Institute of Mathematical Statistics.

[18] Sobol', I. M., "On sensitivity estimation for nonlinear mathematical models," *Matematicheskoe modelirovanie*, Vol. 2, No. 1, 1990, pp. 112–118. Publisher: Russian Academy of Sciences, Branch of Mathematical Sciences.

[19] Blatman, G., and Sudret, B., "Adaptive sparse polynomial chaos expansion based on least angle regression," *Journal of Computational Physics*, Vol. 230, No. 6, 2011, pp. 2345–2367. https://doi.org/10.1016/j.jcp.2010.12.021, URL https://www.sciencedirect.com/science/article/pii/S0021999110006856.